THERMODYNAMICS OF HEAT TURBINES

Jiří Škorpík, skorpik.jiri@email.cz

Author: ŠKORPÍK, Jiří, ORCID: 0000-0002-3034-1696

Issue date: March 2024

Title: Thermodynamics of heat turbines

Journal: Transformační technologie (transformacni-technolgie.cz; fluid-dynamics.education; turbomachinery.education; engineering-sciences.education; stirling-engine.education)

ISSN: 1804-8293

Expansion in heat turbine

Gas expansion in turbines smoothly transforms internal thermal, pressure, kinetic, and potential energy into work. Density and temperature change, necessitating knowledge of *h*-*s* and *T*-*s* diagram design for energy balance calculation.

Usually the expansion is associated with high temperature, at least at the inlet this puts additional special requirements, this time on the blade materials and their cooling.

Adiabatic expansion

Outlet velocity

Comparative change[1.]

In adiabatic expansion, isentropic expansion serves as the ideal comparative change, identifying losses. In ideal expansion, the same exit velocity is usually expected as in actual expansion. This means that the real machine must have larger flow areas than the ideal machine because the loss heat increases the specific volume of the working gas.

Heat transfer

The adiabatic expansion computational model is used in cases where the turbine is not expected to have a significant heat transfer to the surrounding, even if the temperature of the expanding gas is higher than the surrounding temperature, but they are also well thermally insulated and the expansion is too fast to have a significant heat transfer effect on the expansion.

Re-usable heat

h-*s* diagram

T-*s* diagram

Internal losses[1.]

Internal work[1.]

Loss heat

A characteristic feature of expansion in a heat turbine is also the so-called re-usable heat *Δ*. This is a part of the loss heat ([Škorpík, 2024]) generated by dissipation of energy L_q, which was transformed into internal work in another part of the turbine. Figure 1 shows an example of expansion in a turbine or in a single stage in the *h*-*s* and *T*-*s* diagrams. While in the *h*-*s* diagram only the internal losses as a whole can be identified, in the *T*-*s* diagram the individual types of losses can be identified.

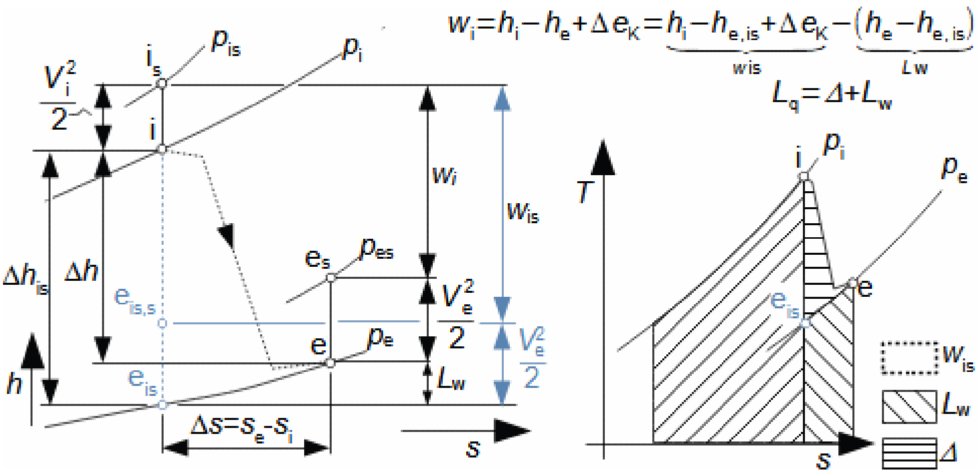

1: Internal work of heat turbine at adiabatic expansion in *h*-*s* and *T*-*s* diagrams

h [J·kg^{-1}] enthalpy; L_q [J·kg^{-1}] loss heat, or sum of different types of energy transformed into internal energy of gas at expansion process; L_w [J·kg^{-1}] internal losses; s [J·kg^{-1}·K^{-1}] entropy; T [K] absolute temperature; w_{is} [J·kg^{-1}] internal work at isentropic expansion (adiabatic expansion with no losses); Δ [J·kg^{-1}] re-usable heat (part of L_q that has been transformed into work in another part of turbine); Δe_K [J·kg^{-1}] difference in kinetic energy between inlet and outlet (usually insignificantly large difference). The index $_{is}$ denotes the isentropic compression states, the index $_s$ the stagnation state. The T-s diagram is constructed when the kinetic energy difference is insignificant. The equations are derived in Appendix 3.

Multi-stage expansion

Reheat factor

The Re-usable heat Δ directly increases the efficiency of multi-stage expansion compared to single-stage expansion, because part of the heat from the loss processes in the previous stage is used in the expansion of the next stage. This means that the internal efficiency of the stage part of multi-stage turbines η_i is greater than the mean internal efficiency of the individual stages η_j, see Figure 2.

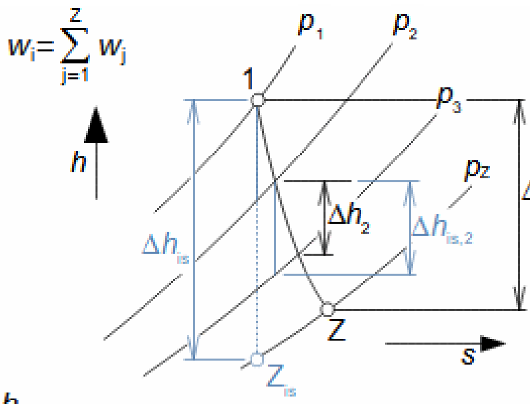

$$1<\frac{\sum_{j=1}^{Z}\Delta h_{is,j}}{\Delta h_{is}}=1+f=\frac{\eta_i}{\eta_j};\quad \eta_i=(1+f)\,\eta_j;\quad 1+f=1-\frac{\Delta}{\Delta h_{is}}+\frac{\sum \Delta_j}{\Delta h_{is}}$$

2: Multi-stage adiabatic expansion in the turbine

Z [-]] number of stages; $1+f$ [1] reheat factor (1.02 to 1.04 according to [Kadrnožka, 1991]); η_i [1] internal expansion efficiency between point 1-Z. The index $_j$ denotes the j-th stage. The equations are derived for the assumption that all stages process the same enthalpy gradient and the expansion is adiabatic. For clarity, the absolute velocity kinetic energy is not plotted in the figure. The equations are derived in Appendix 4.

Polytropic expansion

Polytropic ideal expansion

Heat transfer

The computational model of polytropical expansion is used in cases where the expansion is affected by heat transfer with surrounding. This occurs, for example, in radial turbines with large disk area, in cooling of thermally exposed parts of the turbine, etc. In polytropic expansion, the comparative process is usually reversible polytropic expansion. Polytropic expansion can be described by Equations 3. These equations can be derived from the general equation of the first law of thermodynamics.

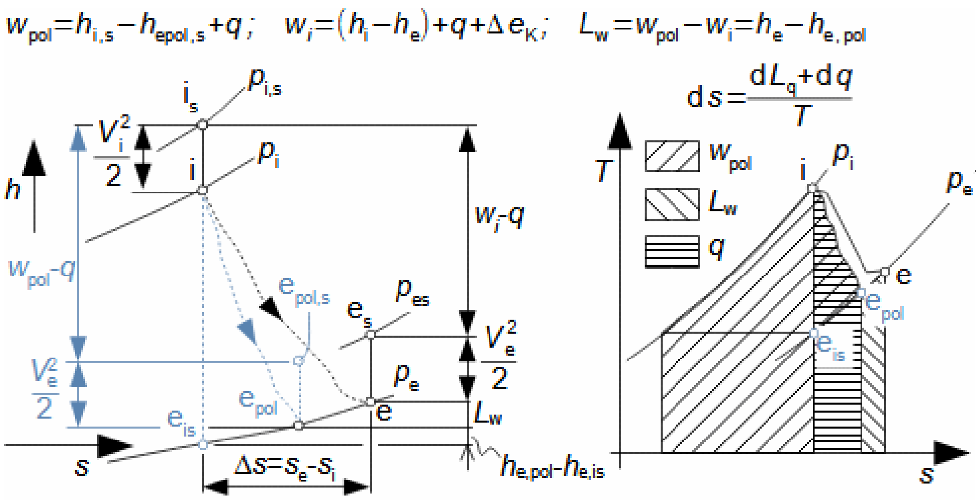

3: Turbine internal work for case $q>0$

e_{pol} state of gas at the machine outlet during reversible polytropic expansion. w_{pol} [J·kg^{-1}] internal work during reversible polytropic expansion (expansion without losses) at same heat transfer with surrounding q - heat q must have the same impact on entropy and temperature as in the actual process. The index $_{pol}$ denotes reversible polytropic expansion. The T-s diagram is constructed when the difference of kinetic energies is insignificant. The procedure for constructing the T-s diagram is described in Appendix 5.

Cooled expansion

Figure 4 shows examples for cooled expansion ($q<0$).

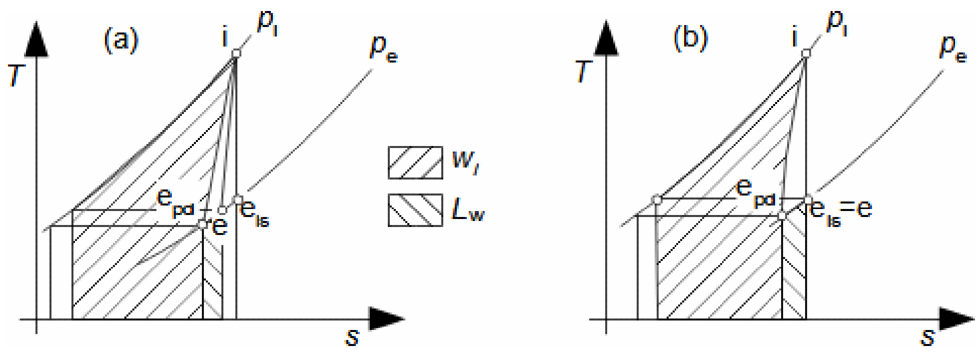

4: Internal work of a turbine with cooled expansion $q<0$

(a) case when $t_{e,is}>t_e$; (b) case when $t_{e,is}=t_e$ (apparently isentropic expansion). The T-s diagram is constructed when the effect of the kinetic energy difference is insignificant.

Thermodynamic calculation of heat turbine stage

For thermodynamic calculations of the heat turbine stage, findings from previous articles in these proceedings can be utilized. Here, only special knowledge on heat turbine stage thermodynamics is summarized and supplemented.

***h-s* diagrams**

Euler work[2.]

Profile losses[4.]

Total losses[5.]

Figure 5 shows the *h-s* diagram of the heat turbine stage at the investigated radius for Euler work caculation. In the case of polytropic expansion, the individual kinetic energy cannot be plotted in the diagrams because the enthalpies are affected by the heat q. The energy balance of the whole stage is shown in blue.

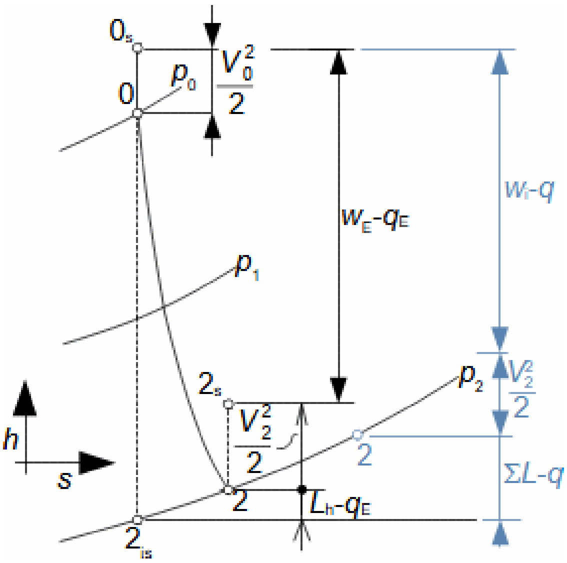

5: *h-s* diagram of expansion in heat turbine stage

L_h [J·kg^{-1}] profile losses;ΣL [J·kg^{-1}] total losses of stage; V [m·s^{-1}] absolute velocity; q_E [J·kg^{-1}] heat transferred in the surroundings of the streamline under investigation.

Straight blades

Axial stage

1D calculation[1.]

Axial stages with straight blades are used as a cheaper alternative to stages with twisted blades, especially in the case of very small ratios of blade length to mean blade diameter [Kadrnožka, 2004, p. 153], i.e. in cases where the spatial character of the flow is not so significant and the use of 1D blade claculation is adequate. Of course, lower efficiency of such stages compared to stages with twisted blades is to be expected. Straight blade stages are used in steam turbines which are manufactured in pieces.

Impulse stage[2.]
Reaction stage[2.]
Reaction[2.]
Dimensionless characteristic[6.]

Straight blade stages are designed with the reaction close to 0 (impulse stages) or with the reaction 0.5 (reaction stages). From the point of view of thermodynamic properties, the differences between these two types of stages can be seen from their dimensionless ψ-ϕ characteristics. Respectively, the impulse stage can be expected to do twice as much internal work as the reaction stage for the same blade length and mean radius and the same rotor speed. On the other hand, the dimensionless characteristic of the impulse stage will be more abrupt than that of the reaction stage, etc.

Impulse stage
Profile losses
Velocity triangle[1.]

Figure 6 shows a typical impulse stage design with reaction of approximately 0.03 to 0.05 and its velocity triangle according [Kadrnožka, 2004, p. 91]. The reaction should be such that it yields a reduction in profile losses, which are a function of velocity, while retaining the benefits of the impulse stage design.

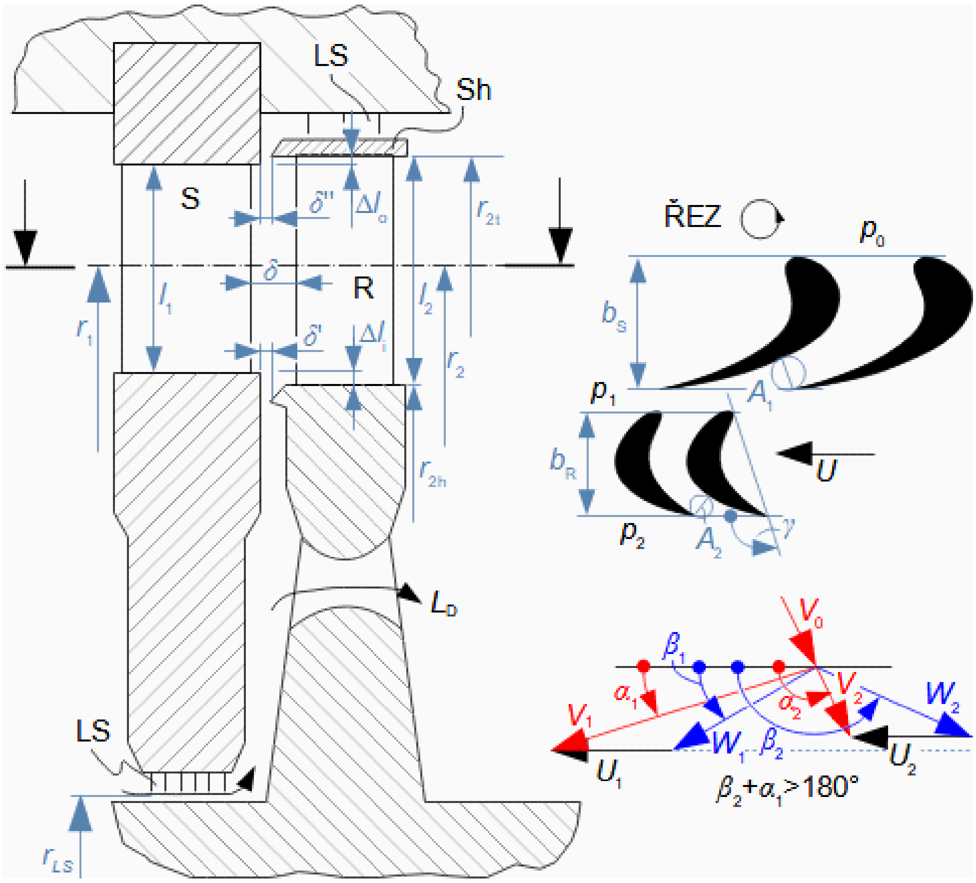

6: Cylindrical cut through axial impulse stage with small reaction and its velocity triangle

Sh-shroud; LS-labyrinth seal. A [m^2] flow area of blade passage; b [m] width of blade row; l [m] length; L_D [kg·s^{-1}] discharge of working fluid from gap between discs (it is loss); r [m] radii of blades (index $_t$ denotes tip of blades, index $_h$ denotes root of blades); U [m·s^{-1}] blade speed; W [m·s^{-1}] relative velocity; α [°] angle of absolute velocity; β [°] angle of relative velocity; γ [°] stagger angle; δ [m] sizes of axial gaps.

Reaction stage
Symmetric blades
Meridian velocity[1]

Figure 7 shows a cylindrical section of the reaction stage and its velocity triangle for reaction R=0.5. In such the reaction, the profile losses are the lowest because the velocities V_1 and W_2 are the same or very similar. Hence the symmetrical shape of the velocity triangle for the stator and rotor blade rows and hence the same blade shape can be used for both stator and rotor rows, which is advantageous for manufacturing. When the symmetry of the velocity triangles is maintained, the condition $V_{2\theta}$=0 cannot usually be met, see Problem 2. The increase in blade length at the outlet is due to the requirement to maintain the meridional velocity as the density decreases during expansion.

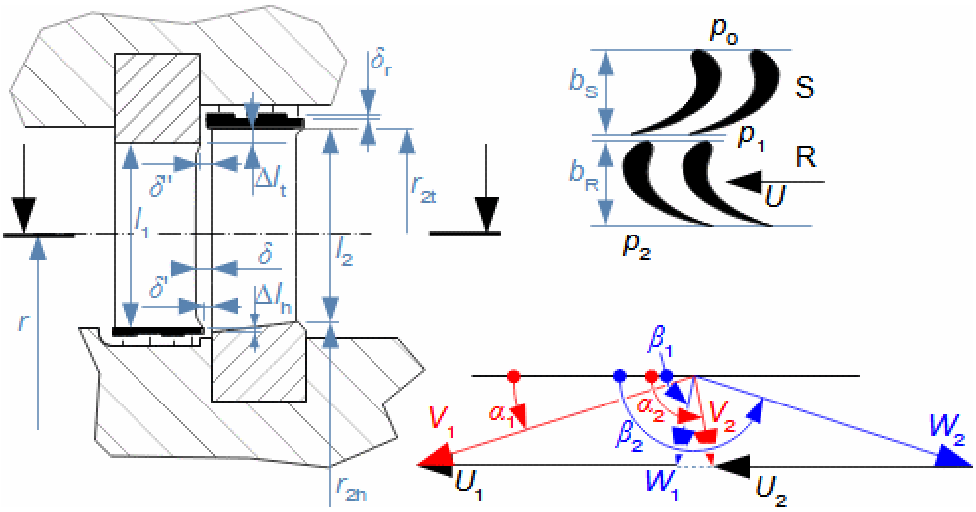

7: Cylindrical cut through axial reaction stage

The blade roots are not drawn in the pictures.

Profile losses
Outlet velocity
Velocity coefficient
Profile cascade[4]

Also typical of straight blades steam turbines is the simplified prediction of the magnitude of the profile losses using nozzle theory instead of using the aerodynamic data of the profile cascades. This prediction consists of matching the blade passage to the nozzle, albeit curved, then the change in exit velocity from the passage and hence the profile loss can be predicted using the velocity coefficient (see the articel Flow of gases and steam through nozzles [Škorpík, 2023]) as shown in Figure 8.

$$L_h^S=\frac{V_{1is}^2}{2}-\frac{V_1^2}{2}=\frac{V_{1is}^2}{2}(1-\varphi^2)$$

$$L_h^R=\frac{W_{2is}^2}{2}-\frac{W_2^2}{2}=\frac{W_{2is}^2}{2}(1-\psi^2)$$

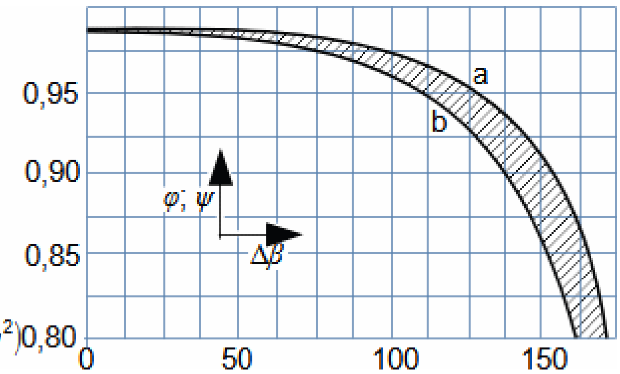

8: Values of velocity coefficients of steam turbine blade rows a-pressure row (reaction 0,5); b-equal pressure row. $\Delta\beta$ [°] angle of camber of flow; φ [1] velocity coefficient in stator passage; ψ [1] velocity coefficient in rotor passage. Index $_1$ indicates parameters upstream of the rotor blade row, index $_2$ indicates parameters downstream of the rotor blade row, index $_S$ indicates the stator blade row, index $_R$ indicates the rotor blade row. Data source [Krbek, 1990, p. 82].

Zweifel coefficient[3].

Such a simplification can also be made for very stagger angle profile cascades, where the density of profile cascade can be determined using the Zweifel coefficient.

Flow coefficient

The nozzle theory can also be used in the determination of the flow coefficient μ (defined in the article Flow of gases and steam through nozzles [Škorpík, 2023]) through the blade passage. For example, in [Kadrnožka, 2004, p. 110] the values of the flow coefficient for different cases of flow in blade rows are given.

Curtis stage

A special case of the impulse stage is the Curtis stage, which is used as a more suitable variant of single-stage heat turbines with a high enthalpy drop. In this case, the available energy is transformed into kinetic energy in the stator row of blades, but then flows through more than one row of rotor blades, between which another equal pressure stator blade is inserted, which only changes the direction of flow, see Figure 9. In the case of very small steam turbines, a reversal passage can also be used whereby the steam passes through the rotor blade row twice, see Figure 10.

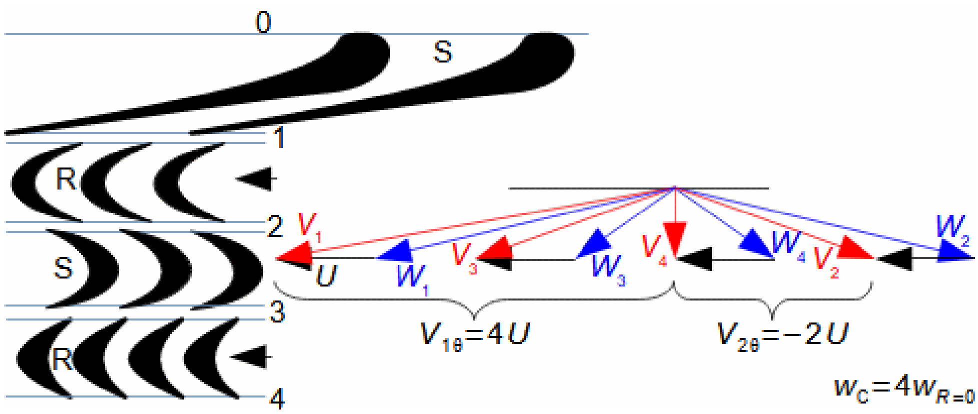

9: The cylindrical section of the Curtis stage and its velocity triangle

Velocity triangle of Curtis stage in this figure is for the case of ideal flow without profile losses. w_C [kJ·kg^{-1}] Euler work of ideal Curtis stage; $w_{R=0}$ [kJ·kg^{-1}] Euler work of ideal impulse stage. The derivation of the ideal Curtis stage Euler work equation is shown in Appendix 7..

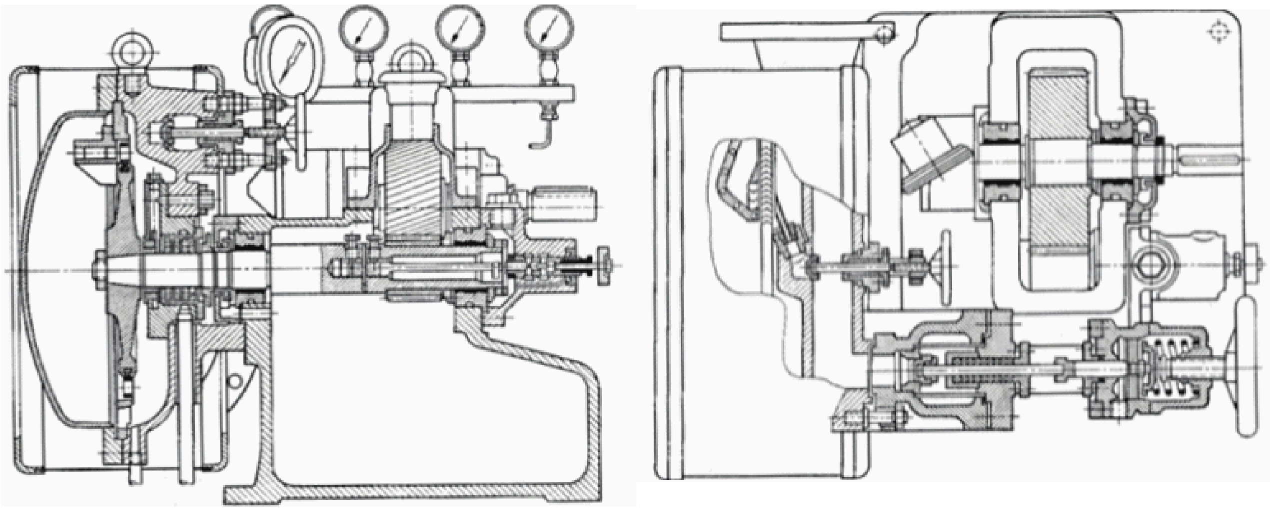

10: Single stage steam turbine for low flow and high enthalpy drop

The turbine is designed as the Curtis stage. The turbine contains only one Laval nozzle. Instead of a second stator row, there is a reversal passage that brings the steam back to the first rotor row. Figure from [Miller et al. 1972, p. 188].

Curtis stage
Impulse stage
Reaction stage

The Curtis stage under the same conditions can handle a larger enthalpy difference in the stage than the impulse or reaction stage (in the ratios of 8:2:1 as shown in the above paragraphs), but at a lower internal efficiency because the velocities, and hence the profile losses, are very high. To increase the internal efficiency at the mean radius of the Curtis stage, individual blade rows are constructed with a slight overpressure.

Impulse stage
Curtis stage
Reaction stage

Impulse stages are used in single-stage turbines called Laval turbines as well as in multi-stage steam and gas turbines. Curtis stages are used where the emphasis is on high power in a small volume. The Curtis stage was the driving turbine of the 50 kW turbopumps of the German V-2 rocket engine, as well as being found in the Russian RD 108 rocket engines for powering Soyuz etc. Reaction stages are more common in multistage steam turbines with an emphasis on simplicity and smaller purchase requirements.

Twisted blades

Twisted blades[5.]

The thermodynamic calculation of the axial stage of a twisted-blade heat turbine is presented in one of the problem assignments in the article Internal losses of turbomachines and their influence on turbomachine calculation. The procedure for calculating the blade height reaction and the types of losses to be taken into account are also described in that article.

Conical stage

Conical stage[5.]

Radial stage[2.]

In conical stages, the flow area changes by varying the height of the blade edges so that the meridional velocity is maintained as the gas expands. Cone stages come in both twisted blade and straight blade designs. *h-s* diagram of the cone stage at the radius under investigation is identical to that of the radial stage.

Straight blade

Multi-stage turbine

The conical stages with straight blades, or beveled blades in Figure 11, are typical of small industrial back pressure steam turbines. In the case of the stages in Figure 11(a), the advantage is that the $l{\cdot}r^{-1}$ ratio decreases and the blades are the same.

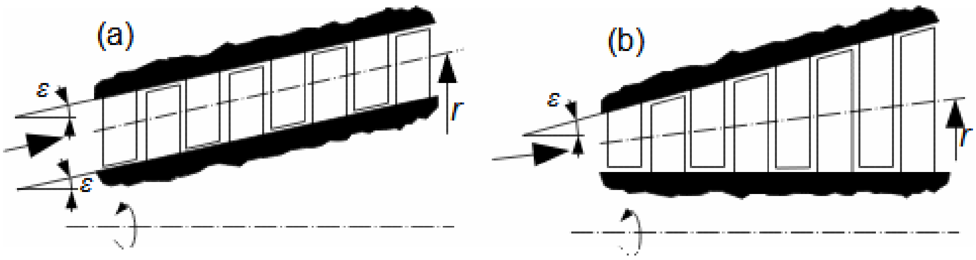

11: Conical stages with straight blades

ε [°] blade cutting at tip and root of blades.

Straight blade

Figure 12 shows the effect of increasing the output radius of the stage in the case of the straight bladed reaction stage of Figure 11. If the blade profile is maintained, the blade speed *U* changes and with it the other velocities, but the angles remain the same. As the blade speeds change, the energy distribution in the stage also changes according to the attached *h-s* diagram, which shows that increasing the blade speed leads to a decrease in the processed enthalpy drop.

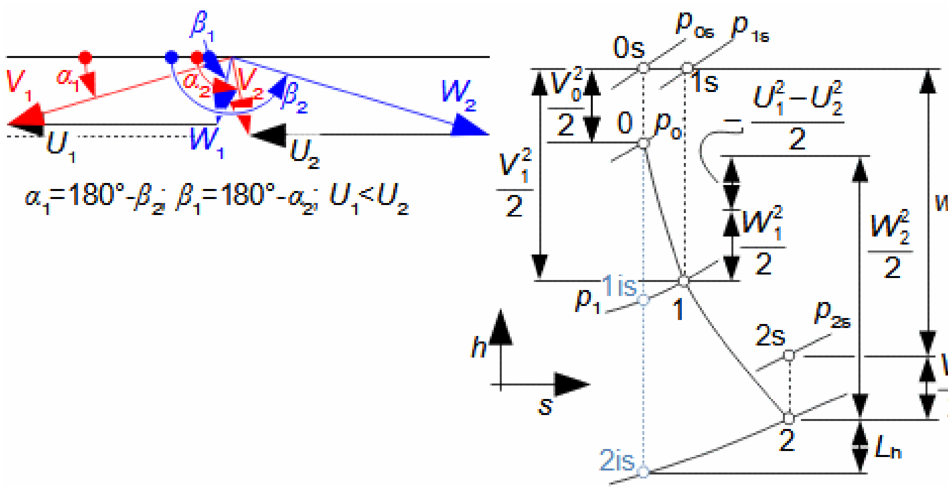

12: Velocity triangle and *h-s* diagram of conical reaction stage with straight blades

Radial turbines

Radial stages are required to have at least a minimum reaction and even equal pressure. For example, for turbines (centripetal stage), a zero reaction stage would result in a deceleration of the relative velocity at the outlet of the rotor row due to centrifugal forces, and therefore to reduce the Euler work. The minimum reaction of centripetal turbines can be determined by imposing the condition $W_1=W_2$.

Radial vs. Axial stages

Steam turbine

Radial stages are used as a more expensive but more efficient single-stage alternative to impulse and Curstis stages, because the Euler work of the radial stage is increased by the tangential velocity difference and so flow velocities can be low even with large enthalpy drop. They are used, for example, in turbochargers and turboexpanders. Radial straight bladed heat turbines are also marginally produced, see Figure 13. These stages are not suitable for water vapour with any moisture content, as the water droplets flow centrifugally due to centrifugal forces.

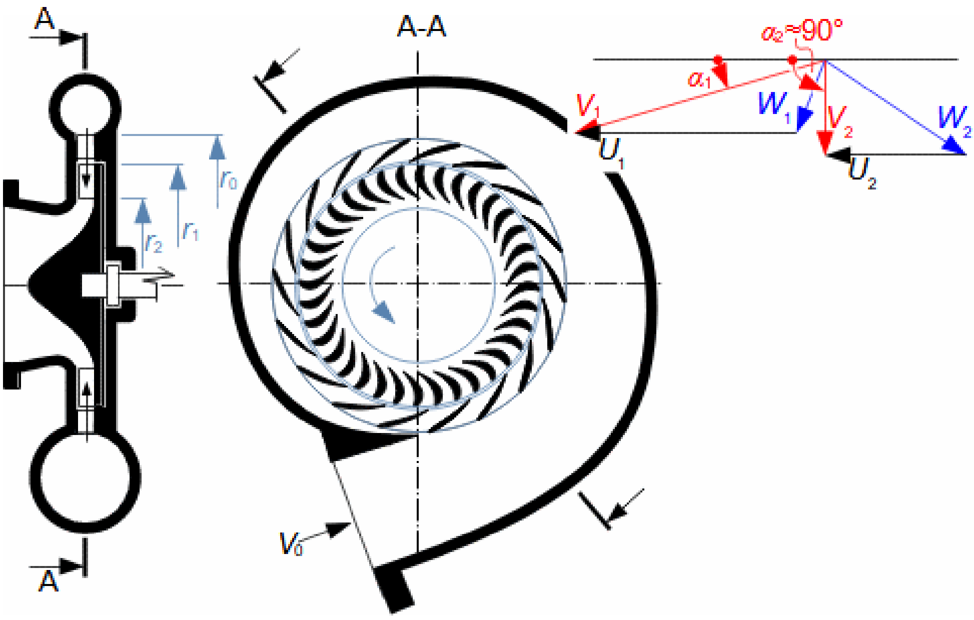

13: Radial single stage steam turbine

Blade cooling performance and methods to increase blade temperature stability

The high temperature of the working gas also allows for high thermal efficiency of the cycle in which the turbine operates. However, this places high demands on the blade material and surface treatment. Another possibility is to cool the blades.

Materials of blades
Temperature stability
Steel
Ingredients
Rotor

At high temperatures, steel strength and modulus of elasticity drop while susceptibility to corrosion rises - the effect of temperature on these material parameters is referred to as temperature stability. Ensuring steel strength at high temperatures involves various blade material ingredients, as depicted in Figure 14 for desired operating temperatures. The alloy compositions of steels for rotors and blades of high temperature heat turbines are given in [Beneš et al., 1974, p. 194], [Koutský, 2005, p. 61], [Škopek, 2007, Appendix 20].

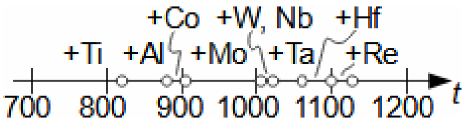

14: Necessary ingredients of blades materials according operating temperature

t [°C] operating temperature of blades. According to data from [Anon., 2014].

Ingredients
Abrasion
Titan
Blade root
Protective coating
Steam turbine blade

The use of admixtures is primarily intended to improve temperature resistance, but will usually degrade other properties of the steel, such as abrasion resistance. For example, Figure 15 shows a steam turbine blade made of a steel-titanium alloy, which reduces the density of the blade and hence the stress from centrifugal force. The disadvantage is the reduction of the surface abrasion resistance, so a protective coating of harder metal is welded onto the blades using a laser (in the picture the blade is still without the protective coating) [Míšek, 2014].

15: Steam turbines blade made of steel and titanium alloy

Doosan Škoda Power 1375 mm steam turbines last stage blade.

CMC

Ceramic matrix composite (CMC) materials based on ionic bonds, which are produced as a single crystal, are also used to increase the high temperature stability of the blades. This material also has a relatively low density, which reduces stresses in the blade from centrifugal forces [Hocko, 2012, p. 55].

Polishing

Surface treatments such as polishing can in turn increase corrosion resistance. Especially at high temperatures in the presence of oxygen, there is a risk of increased scale formation (formation of hard oxides - rust).

Blade cooling
Blade roots
Cooling passages
Boundary layer cooling

If high-quality materials aren't enough, especially for initial heat turbine stages, blades require active cooling. This can involve cooling blade roots, entire blades via passages (Figure 16), or using a film of cold gas blown into the boundary layer through small holes on the pressure or suction side. Air (for combustion turbines) or water (for steam turbines) serves as the cooling medium [Miller et al., 1972, p. 931]. Some early combustion turbine blade cooling concepts, though unsuccessful, are discussed in [Dokoupil, 2015, p. 221].

Air cooling
Anti-corrosion coating
Combustion turbines
Thermal conductivity
Ceramic coatings

For air cooling, cooling passages need anti-corrosion coating. In combustion turbines, cooling air is drawn from the compressor section at slightly higher pressure than around the blade to be cooled. It exits through holes in the blade's trailing edge into the exhaust stream. The cooling efficiency is increased by the outer surface layer of the blades with a low thermal conductivity value, such as ceramic coatings, etc.

16: GE MS5002 series combustion turbine blades with cooling passages [Anon., 2011]

Entalpic drop
First stages
Steam turbines

It is typical for the enthalpy drop distribution in a heat turbine that the first stages are designed to process a larger enthalpy drop than the next stages. While this may degrade the thermodynamic efficiency of the first stages, it will reduce the number of stages operating in the high temperature region and hence the cost of the turbine - such a distribution of enthalpy drops is common in steam turbines.

Problems

Problem 1:

Adiabatic expansion
Steam turbine

Calculate the internal power of Steam turbines and the dryness of steam at the end of expansion. The steam flow through the turbine is 33 t·h^{-1}, the internal efficiency of the turbine is 75%, the specific isentropic work of the turbine is 1259.59kJ·kg^{-1}, the pressure at the turbine outlet is 3 kPa, at the turbine inlet are 3.5 MPa at temperature 450 °C. The solution to the problem is shown in Appendix 1.

§1	entry:	m; η_{is}; w_{is}; p_e; p_i; t_i	calculation:	h_e
§2	calculation:	w_i; P_i	read off:	x_e
§3	read off:	h_i		

Symbol descriptions are in Appendix 1.

Problem 2:

Reaction stage

Design the straight blade lengths, velocity triangles and calculate the axial force acting on the rotor of the reaction stage of steam turbines. The steam flow rate through the stage is 12 kg·s^{-1}, rotor speed is 50 s^{-1}, steam pressure at the stator inlet is 1.25 MPa and temperature is 320 °C, mean diameter of the blade length is 650 mm, reaction is 0.5, the absolute velocity angle at the stator outlet is 20°, the stator and rotor velocity coefficient is the same 0.93. The isentropic drop of the stage shall be 21.3 kJ·kg^{-1}. Compare the pressure coefficient with the pressure coefficient for an ideal reaction stage. The solution to the problem is shown in Appendix 2.
The problem is taken from [Krbek, 1990 p. 110].

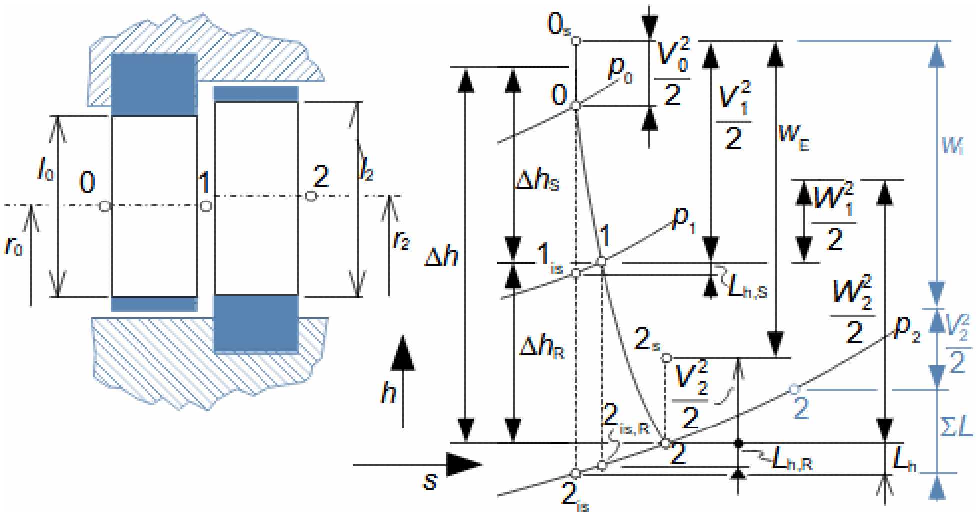

§1	entry:	m; N; p_0; t_0; d_{ref}; R; α_1; φ, ψ; Δh_{is}		read off:	p_1; s_1; h^R_{2is}
§2	read off:	v_0; s_0; h_0		calculation:	h_2; L_h
	calculation:	$h_{2,is}$; U		compare:	L_h z §5 vs. L_h §3
	read off:	p_2	§6	calculation:	V_a, W_a; $V_{1\theta}$; $W_{1\theta}$; β_1; α_2; β_2
§3	estimate:	$\sim\eta_E$	§7	read off:	v_1; v_2
	calculation:	w_{Eis}; w_E; L_h; h_2		calculation:	l_1; l_2
	read off:	s_2	§8	calculation:	F_a
§4	calculation:	Δh_R; V_1, W_2; V_0, V_2, W_1	§9	read off:	ψ_{id}
§5	calculation:	L^S_h, L^R_h; h_{0s}; h_1; h_{1is}		calculation:	ψ

Symbol descriptions are in Appendix 2.

References

ŠKORPÍK, Jiří, 2023, Flow of gases and steam through nozzles, *Transformační technologie*, Brno, [online], ISSN 1804-8293, https://fluid-dynamics.education/flow-of-gases-and-steam-through-nozzles.html#flow-through-nozzle-with-losses.

ŠKORPÍK, Jiří, 2024, Technická termomechanika, *Transformační technologie*, Brno, ISSN 1804-8293, https://engineering-sciences.education/technicka-termomechanika.html.

ANON., 2011, *MS 5002 Gas Turbine a Through D Evolution*, ge.com.

ANON., 2014, Co nám může v budoucnosti nejvíc chybět? Na čem jsem závislí, *Technický týdeník*, 01/2014, Business Media CZ, Praha, ISSN 0040-1064.

BENEŠ, Antonín, DRASTÍK, František, HOSTINSKÝ, Zdeněk, KOUTSKÝ, Jaroslav, NĚMEC, Josef, 1974, *Nauka o kovech*, SNTL, Praha.

DOKOUPIL, Eduard, 2015, *Turbíny pro Luftwaffe: zrod a popis prvních německých proudových motorů*, Dokoupil Eduard, Světlá, ISBN 978-80-260-8153-1.

HOCKO, Marián, 2012, *Transformace leteckých lopatkových motorů na spalovací turbíny*, Západočeská univerzita v Plzni, Plzeň, ISBN 978-80-261-0218-2.

KADRNOŽKA, Jaroslav, 1991, *Teorie lopatkových strojů*, Vysoké učení technické v Brně, Brno, ISBN 80-214-0275-X.

KADRNOŽKA, Jaroslav, 2004, *Tepelné turbíny a turbokompresory*, Akademické nakladatelství CERM, s.r.o., Brno, ISBN 80-7204-346-3.

KOUTSKÝ, Jaroslav, 2005, Development and application of Original Special Steels-Base of World Famous Level of Skoda-Works Steam turbines, *Energetické stroje-termomechanika-mechanika tekutin* , Fakulta strojní Západočeské university v Plzni, Plzeň.

KRBEK, Jaroslav, 1990, *Tepelné turbíny a turbokompresory*, Vysoké učení technické v Brně, Brno, ISBN 80-214-0236-9.

MILLER, Rudolf, HOCHRAINER, A., LÖHNER, K., PETERMANN, H., 1972, *Energietechnik und Kraftmaschinen*, Rowohlt taschenbuch verlag GmbH, Hamburg, ISBN 3-499-19042-7.

MÍŠEK, Tomáš, 2014, Vývoj ultra dlouhé lopatky Doosan Škoda Power pro kondenzační Steam turbines, *Technický týdeník*, 10/2014, Business Media CZ, Praha, ISSN 0040-1064.

POLSTER, Burkard, 2014, *Q.E.D. Krása matematického důkazu*, Dokořán s.r.o., Praha, ISBN 978-80-7363-532-9.

ŠKOPEK, Jan, 2007, *Parní turbína-tepelný a pevnostní výpočet*, Západočeská univerzita v Plzni, Plzeň, ISBN 978-80-7043-256-3.